European Rotorcraft Forum

MORPHING HELICOPTER ROTOR BLADE WITH CURVILINEAR FIBER COMPOSITES

M. Senthil Murugan[1], Benjamin K. S. Woods and Michael. I. Friswell

College of Engineering, Swansea University, Singleton Park, Swansea SA2 8PP, UK

Abstract

A variable camber morphing rotor blade with curvilinear fiber composite skin is studied in this paper. The benefits of curvilinear fiber (CVF) composites for morphing skin over the linear fiber are investigated, initially. The skin of a morphing blade is modeled as a plate supported between the D-spar and trailing edge of typical rotor blade dimensions. The CVF composite shows about 60 % increase in the in-plane to out-of-plane bending deformation ratio compared to composites with linear fiber paths. In the second step, a previously developed biologically inspired variable camber internal structure is investigated for variable camber rotor blade. A fluid-structure interaction simulation is performed to obtain the aerodynamic loads acting on the skins of the variable camber internal structure proto type model. The upper skin of this prototype is modeled and optimized to find the optimal curvilinear fiber paths. The ply angles between the stringers are optimized to minimize the strain energy required to deform the skin for camber change and minimize the maximum out-of-plane deflection. The optimal results show that the plies which are away from neutral axis play a significant role in minimizing the out-of-plane deflections. The plies near to the neutral axis play a considerable role in minimizing the strain energy. Further, the skin requires the stiff plies near the D-spar and a flexible plies near the trailing edge tip as the pressure load decreases from the quarter chord to trailing edge portion of the airfoil. The numerical results show that the CVF composite skins can decouple the in-plane and out-plane requirements of morphing skins. The CVF composite skins show considerable reduction in the actuation energy while simultaneously minimizing the skin out-of-plane deformation requirements.

[1] Post Doctoral Research Assistant; Corresponding author; E-mail: s.m.masanam@swansea.ac.uk; Address: College of Engineering, Swansea University, Swansea, UK;

1. INTRODUCTION

Morphing rotorcraft concepts aim to expand the flight envelope by designing blades that can reconfigure to an optimal shape in flight [1,2]. This reconfiguration can increase the payload, fuel efficiency, range, maximum speed and altitude, and also reduce the vibrations and noise more efficiently when compared to rotor blades with a fixed geometry. The morphing structures can be categorized as large, medium and small scale morphing structures. The variable camber rotor blade is a small scale morphing concept which requires the structures to undergo a strain of around 2-3% [3].

Aerodynamic aspects of variable camber leading edge design based on complaint structures technology for dynamic stall control were studied by Kerho[4]. Gandhi et al.[3] performed an optimization study to design the rib of a controllable camber rotor airfoil for helicopter vibration reduction. However, the skin was based on an isotropic material with a constant thickness in the optimization procedure. The above studies mainly focused on designing the skins made of isotropic materials for variable camber applications.

Thill et al.[5] reviewed various materials for morphing skins. One candidate for the morphing skins of variable camber airfoils is the curvilinear fiber composite. In curvilinear composites, the fiber angle is varied spatially in contrast to the conventional spatially constant fiber angle composites. This curvilinear nature can be utilized to design the composites with low in-plane stiffness while retaining a high out-of-plane bending stiffness. Very few studies have focused on the use of curvilinear fiber (CVF) composites for variable camber applications. Thuwis et al.[6] performed an optimization study with CVF composites for a leading edge skin of a fixed wing. The study concluded that the use of CVF composites increased the design space of compliant morphing wing skins. However, as far as the author knows, no study has focused on the use of CVF composites for the variable camber morphing rotor blade.

The aim of this present work is to design the trailing edge of a variable camber rotor blade with a smooth and aerodynamically efficient compliant skin made of curvilinear fiber composites. An optimization framework is developed to find the optimal distribution of skin stiffness by spatially varying the fiber angles. The out-of-plane bending stiffness is maximized to withstand the aerodynamic loads while the in-plane stiffness is minimized simultaneously to reduce the strain energy by camber variation of the trailing edge which is proportional to actuation energy. The structural analysis is performed with Finite element Method (FEM).

2. CURVILINEAR FIBER COMPOSITE SKINS

In general, the conventional blade skins are made of balanced symmetric laminates to avoid undesired elastic couplings. For a balanced symmetric laminate with curvilinear fiber angles, the constitutive equations can be given as

$$\begin{Bmatrix} Nx \\ Ny \\ Nxy \end{Bmatrix} = \begin{bmatrix} A11(x,y) & A12(x,y) & 0 \\ A12(x,y) & A22(x,y) & 0 \\ 0 & 0 & A66(x,y) \end{bmatrix} \begin{Bmatrix} Uo,x \\ Vo,y \\ Uo,y + Vo,x \end{Bmatrix} \quad \textbf{(1)}$$

$$\begin{Bmatrix} Mx \\ My \\ Mxy \end{Bmatrix} = \begin{bmatrix} D11(x,y) & D12(x,y) & D16(x,y) \\ D12(x,y) & D22(x,y) & D26(x,y) \\ D26(x,y) & D26(x,y) & D66(x,y) \end{bmatrix} \begin{Bmatrix} Wo,xx \\ Wo,yy \\ 2Wo,xy \end{Bmatrix}$$

where A_{ij} and D_{ij} are the elements of the in-plane and bending stiffness matrix of the composite plate, respectively[7]. The curved fiber composite is shown in Fig.1. The mid out-of-plane displacement is represented by *w* and in-plane displacements in the x and y directions are represented by *u* and *v*, respectively. The above equations show that the in-plane and out-of-plane displacements are in-dependent and depend on A_{ij} and D_{ij}, respectively. These stiffness parameters can be given as

$$Aij = \sum_{k=0}^{n} Qij \quad (Zk - \quad Zk-1) \quad \textbf{(2)}$$

$$Dij = \sum_{k=0}^{n} Qij/3 \quad (Zk^3 - \quad Zk-1^3)$$

where Q_{ij}'s are the elements of the transformed reduced stiffness matrix, Z_k and, Z_{k-1} are the upper and lower coordinates of the k^{th} ply. The above relations show the in-plane stiffness of CVF laminate is a function of the spatial variation of fiber angle and thickness of the plies. Similarly, the bending stiffness of a CVF laminate is a function of the spatial variation of fiber angle and stacking sequence of plies in addition to its thickness.

The fiber paths of a variable stiffness composite plate can be defined in multiple ways. However, the fiber paths are limited by the manufacturing constraints. Most of the studies on curved fiber composite define a linear, 1-D variation of a reference fiber path. This linear variation along the panel direction y can be given as

$$\theta(y) = 2(T_1 - T_o)|\frac{y}{b}| + T_o \quad (3)$$

where $\theta(y)$ represents the fiber orientation, b denotes the width of the plate, T_1 and T_0 represent the fiber angles at the edge ($y = b/2$) and middle of the plate ($y = 0$), respectively. This reference fiber path, as shown in Fig. 1, can be repeated along the x direction to manufacture the CVF composite plate. The fiber path definition of the single ply layer is generally represented as (T_0/ T_1) and the numerical values are given in degrees.

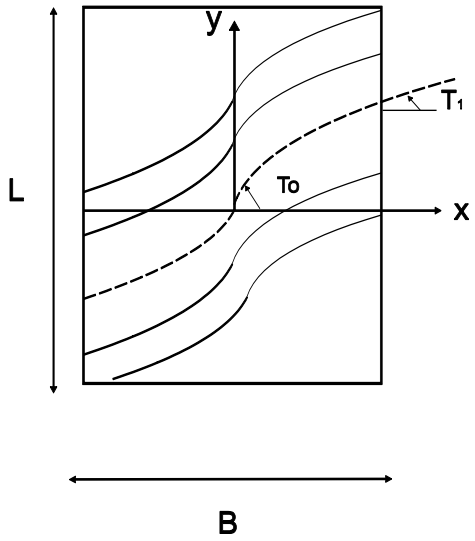

Fig.1 Curved fiber composites

In this section, a morphing wing skin idealised as composite plate is studied to investiage the benefits of CVF for camber morphing or chord extension type wing morphing. However, in the later sections, the variable camber rib and skin of a specific rotor blade is studied.

A morphing aircraft based on the variable chord or variable camber concepts require wing skins with low in-plane stiffness to allow a large in-plane deformation and high out of plane bending stiffness to carry the aerodynamic loads. For example, a typical a rotor blade with possible chord extension is shown in Fig. 2. The wing skin extends from an initial position $ABCD$ to $ABEF$. This portion of the wing skin can be modeled as a composite plate with boundary conditions approximately representing the wing skin. The skin is modeled as simply supported at three sides and fixed at one side. The morphing wing skins are subjected to the aerodynamic loads and the actuation forces as shown in Fig. 3. A uniform pressure which represents the aerodynamic pressure is applied in the XY plane. Similarly, a uniform in-plane load to represent the actuation force is applied along the boundary CD of the plate as shown in Fig. 3.

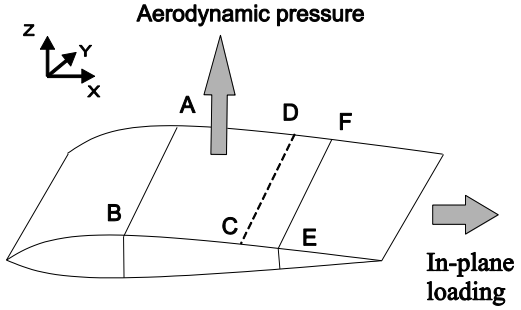

Fig.2 Wing morphing

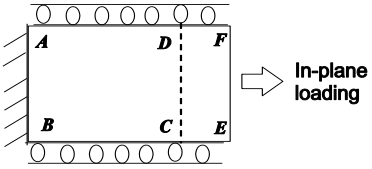

Fig.3a In-plane loading boundary conditions

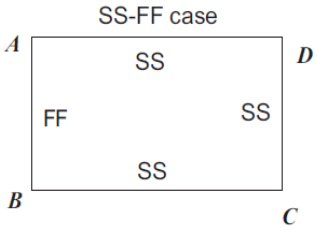

Fig.3b Out-of-plane loading boundary conditions

The in-plane and out-of-plane deformations of the plate corresponding to these loads are measured as the fiber angles vary. That is the T_0 and T_1 values are varied from 0 to 90 deg. A graphite/epoxy laminate with 8 plies is considered. Each ply thickness is 0.025 mm. The structural analysis is carried out with shell elements in ANSYS.

An increase in the in-plane area δA ($CDEF$) for a prescribed in-plane loading is measured as shown in Fig. 3a. The morphing wing skins also require a minimum out-of-plane deformation to retain the aerodynamic performance of the wing. Therefore, the maximum value of out-of-plane deformation (w_{max}) for a prescribed uniform pressure loading is measured.

The ratio of change in the in-plane area (δA) to the maximum out-of-plane direction (w_{max}) can be used to measure the performance of the CVF composites. This ratio is defined as the flexibility ratio (FR = $\delta A/w_{max}$). A higher FR can be considered as

optimal for the morphing skin requirements. The flexibility ratio is normalized with the values corresponding to a baseline plate with *±45* deg straight fibers (*FR= FR$_b$*) to measure the benefits of CVF over straight fibers. The skins are generally supported along the span length which is generally higher than the chord length. Therefore, an aspect ratio (AR) of 2.0 is considered. The non-dimensionalised values of FR for T_0 and T_1 vary from 0 to 90 degrees (deg) are shown in Fig. 4. The corresponding optimal curved fibres for maximum FR are shown in Fig. 5

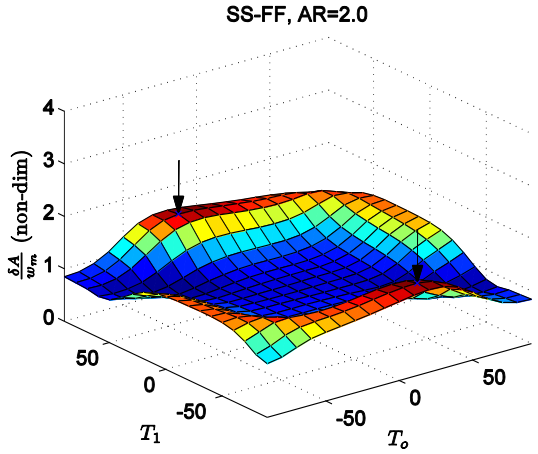

Fig.4 Variation of FR of the plate with curved fiber paths and the optimal fiber paths for aspect ratio 2.0

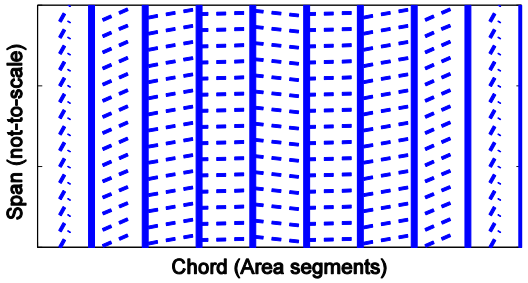

Fig. 5 Variation of FR of the plate with curved fiber paths and the optimal fiber paths for aspect ratio 2.0

The CVF shows an increase of 100% in FR when compared to the baseline with straight fibers. This numerical result shows that the curved fibers have considerable influence on the in-plane flexibility and out-of-plane bending.

3. VARIABLE CAMBER STRUCTURE

In the previous section, the skin is modeled as a plate supported between the D-spar and trailing edge tip portion. However, a proper representation of the internal structure for a variable camber morphing rotor blade is discussed in this section. The rib structure or the internal structure below the skin which transfers the aerodynamic load to the D-spar which is main load carrying member plays a major role in morphing rotor blade. The rib structure has to be capable of transfering the aerodynamic loads as well as the actuation mechanism to deform the blade.

3.1 FishBAC Concept

Woods and Friswell studied a novel airfoil morphing structure known as the Fishbone Active Camber (FishBAC) structure[8]. This design employs a biologically inspired compliant structure to create large, continuous changes in airfoil camber and section aerodynamic properties[7]. In this study, the FishBAC is used as the internal structure to realize the variable camber morphing rotor blade. A schematic overview of the FishBAC concept is shown in Figs. 6.

The FishBAC structure consists of a thin chordwise bending beam spine with stringers branching off to connect it to a pre-tensioned Elastomeric Matrix Composite (EMC) skin surface. Smooth, continuous bending deflections are driven by a high stiffness, antagonistic tendon system. Actuators mounted in the D-spar drive a tendon spooling pulley through a non-backdrivable mechanism (such as a low lead angle worm and worm gear). Rotation of the pulley creates equal but opposite deflections of the tendons. These differential displacements generate a bending moment on the rigid trailing edge strip, which then induces bending of the trailing edge morphing structure to create large changes in airfoil camber. Since the tendon system is non-backdrivable, no actuation energy is required to hold the deflected position of the structure, leading to increased operational efficiency.

The FishBAC concept creates large camber deflections with minimal actuation energy requirements through the use of structural and material anisotropy. The spine and stringer core is highly anisotropic, with very low bending stiffness along the chord direction, but high spanwise and through-thickness bending stiffness. That is, the bending stiffness corresponding to the camber variation is less while the blade bending stiffness along the span wise direction is high.

A curvilinear fiber orientation, as discussed in the previous section, would allow for de-coupling of the in-plane stiffness and the out-of-plane stiffness. Chordwise alignment of CVF allows them to bridge between stringers, providing significantly increased out-of-plane stiffness compared to 90° fibers of the baseline, while the high curvature allows for a non-linear in-plane deformation mechanism. With a sufficiently shear compliant matrix (such as an elastomer), the fibers are able to first deform in a

straightening mechanism before being directly strained themselves. Therefore, a CVF skin with FishBAC internal structure can be beneficial in realizing the variable camber morphing blade

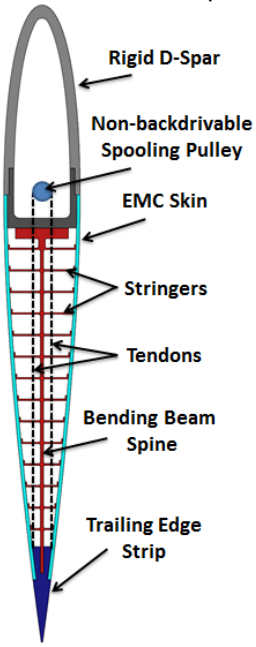

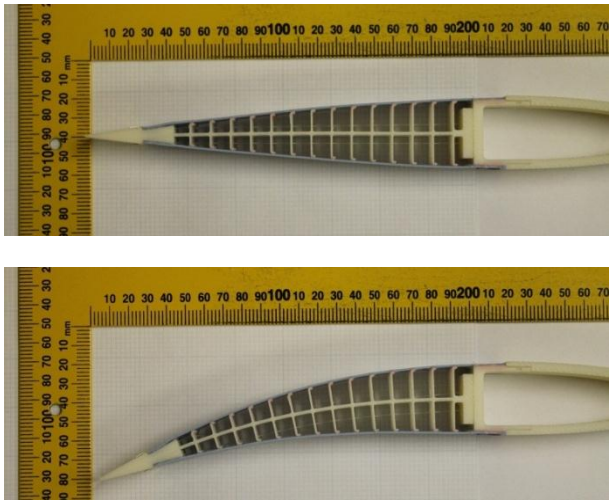

Fig. 6 FishBAC internal structure

3.2 Fluid Structure Interaction

The deflected FishBAC skin surface shape and pressure loadings used in the optimization of skins, in the later section, are generated by a fully coupled Fluid Structure Interaction (FSI) analysis. The FSI is performed with parameters of 0.3 m chord, 2D FishBAC airfoil operating at M = 0.3 and 10 degrees angle of attack. Full details of the operating point and the resulting aerodynamic coefficients are shown in Table 1.

Table 1. FishBAC FSI solution parameters

Parameter	Value	Units
Baseline airfoil	NACA 0012	NA
Chord	0.3	m
Mach #	0.3	NA
Reynolds #	1,000,000	NA
P_{atm}	101,325	Pa
Angle of attack	10	degrees
Drive pulley rotation	30	degrees
Lift coefficient	1.70	NA
Drag coefficient	0.061	NA
Moment coefficient	-0.063	NA

The FSI code, developed by the second author, finds the converged static equilibrium deflections of the structure under actuation and aerodynamic loading. The algorithm of the FSI code will be briefly overviewed here to provide sufficient understanding of the aerodynamic results used in the optimal design of curved fiber skins.

The FishBAC structure's chordwise bending stiffness is captured using an Euler Bernoulli beam analysis. The spine is modelled as a simple beam, and the stringers are assumed to have negligible impact on chordwise bending stiffness. The in-plane skin stiffness contribution to the global bending stiffness is included as a linear superposition onto the bending spine using the parallel axis theorem. The tendon driven actuation is included by modelling the tendons as linear elastic axial beams with an intial prescribed displacement and no bending stiffness. The inboard deflections of the tendons are prescribed by the rotation angle of the spooling pulley. While the tendons do not have any bending stiffness of their own, they are held at a constant distance from the bending spine as the trailing edge morphs by traveling through small orifices in the stringers. Due to their constant distance from the neutral axis, tendon strains induced by structural bending can be derived from Euler Bernoulli theory as well. The axial stiffness and initial displacement of the tendons will therefore drive the trailing edge deflections by creating bending moments on the trailing edge strip (where they are anchored) which are equal to the sum of the axial forces in the tendons times their distance from the neutral axis.

The effects of aerodynamic loading on the structure are included through XFOIL calculations of the aerodynamic pressure distributions. At each iteration step, the pressure acting on the current predicted deflection is calculated and applied as a continuously variable pressure distribution on the structure. Integrating the pressure distribution along the chord according to Euler Bernoulli theory, and with an additional tip moment added for the tendon

actuation effects, the stiffness distribution of the structure produces a cambered displacement profile for the airfoil. The analysis is iterated until a converged solution is achieved, with actuation, aerodynamics and structural stiffness producing a net equilibrium. Convergence is monitored through the magnitude of spine displacement and the aerodynamic coefficients: convergence is only achieved when the tip deflection, lift coefficient, drag coefficient, and moment coefficient of the FishBAC are found to change less than 2% between iterations.

4. VARIABLE CAMBER SKINS

In this section, the skins for variable camber airfoil section with FISHBAC internal structure is studied. The deflections caused by the aerodynamic pressure can play a significant role in controling the flow over the airfoil. Similarly, the increase in actuation power requiremenrs can increase in the weight penalities of rotor blade. Minimizing the power or actuation requirements for morphing can result in siginifcant weight savings. Therfore, the objective is to design the skin to minimize the actuation energy while simultaneously minimizing the out-of-plane deflections caused due to aerodynamic pressure.

4.1 Structural Model

The FishBAC internal structure shown in the previous section has 14 stringers along the chord wise direction. The FishBAC protoptype dimensions are used in the structual analysis. In theoertical simulations, the skin is modeled as a shell which is simply supported over the stringers. This allows the skin to deform in the chordwise direction while supported in the out of plane direction by the stringers as shown in Fig. 7. The trailing edge and leading edge portions of the skin are modeled as clamped supports.

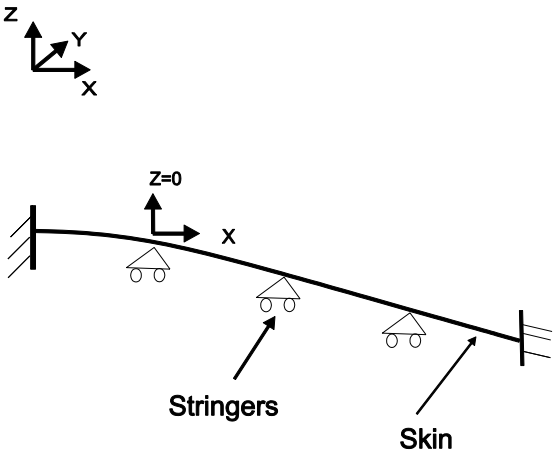

Fig. 7 Boundary conditions of skin and stringers

The airfoil is allowed to vary from the NACA 0012 initial configuration to a converged cambered configuration obtained from the FSI simulations. The net pressure (aerodynamic - atmospheric) acting on the upper skins along the chord is calculated with the FSI simulations are shown in Fig. 8.

The pressure distribution shows that each panel between the stringers has a different pressure distribution. Similarly, the induced strain energy also varies with each panel while varying the stiffness of each panel. Therefore, the variation in strain energy and pressure requirements of each panel requires skins with different ply angle values. By designing the variation of fiber angles along the chord, the actuation energy required to vary the camber and maximum out-of-plane deflections can be minimized.

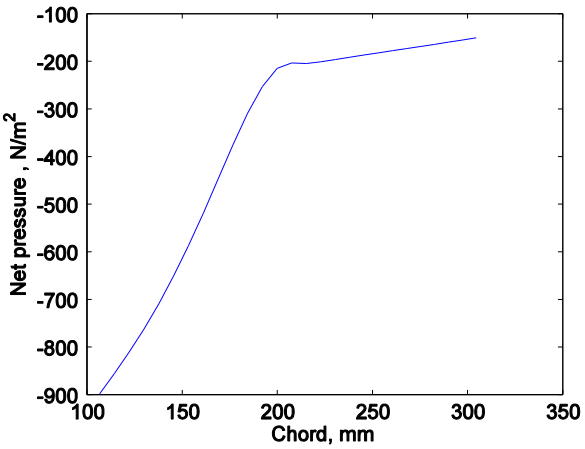

Fig. 8 Net pressure distribution on the upper skin

4.2 Optimization

The optimization is carried out as a three step process. In the first step, the skin is modeled with zero camber. The prescribed deformation due to change in the camber is applied to the initial configuration as shown in Fig. 9. That is, the prescribed deflections of each of the stringer connections are applied. The strain energy stored in the skin due to this deformation is calculated. This strain energy is considered to be proportional to the actuation energy needed to deflect the skin.

In the second step, the net pressure is applied to the deflected skin from the previous step. The vertical deflections of the stringers are constrained as shown in Fig. 7. The maximum deflections of the skin between the stringers are measured. The strain energy and maximum deflections are then passed to the optimization algorithm for fitness function evaluation. The optimization problem can be defined as

$$\text{Minimize, } F = \max\left[J_1(\boldsymbol{X}), J_2(\boldsymbol{X})\right]$$

where $\boldsymbol{X}$ is the vector of design variables or ply angles, J_1 is the strain energy and J_2 is the maximum out-of-plane deflection of the skin panels. Here, the objective functions are non-dimensionalized with the strain energy and maximum out-of-deflection values corresponding to the skin with *±45* deg linear fiber laminate.

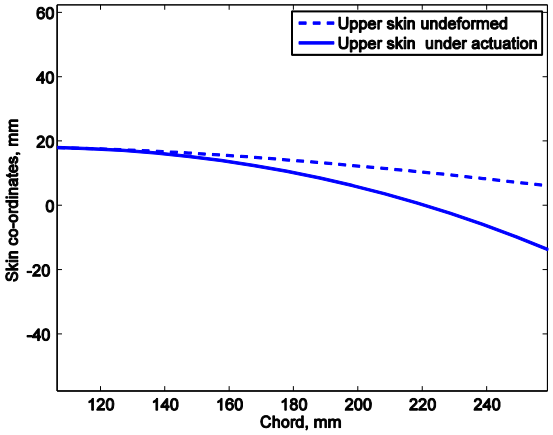

Fig. 9 Upper skin deformations under actuation forces

Before the optimization, the strain energy induced in the skin due to the change in the camber is calculated for ply angles (linear fibers) varying from 0 to 90 deg. The strain energy (SE) varies from 3.25 to 0.25 J as the angle varies from 0 to 90 deg. The SE shows a much smaller value (0.25 J) for ply angles greater than 45 deg compared to 0 deg. A servo actuator capable of providing 2.5 J and dimensions to fit in the FishBAC will be used for actuation in the future studies.

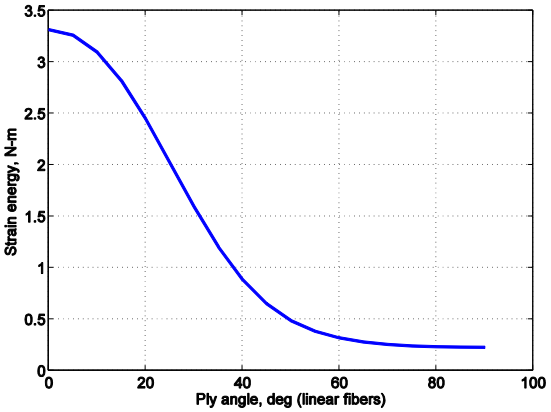

Fig. 10 Strain energy of skin due to camber variation

The optimization is carried out with three cases for the representation of the ply angles. The skin is considered to be made of a graphite/epoxy balanced symmetric laminate with 16 plies. Each ply has a thickness of 0.0125 mm. The optimization performed with various ply angle representations and loading conditions are discussed in the following:

Case I: In this case the fibers are considered to vary along the chord direction. That is the fiber paths along the 14 panels are represented with two design variables T_0 and T_1. However, the ply angles of each panel are given by equation (3). The plies along the thickness are considered to be different. This case results in the 8 design variables given below.

$$\boldsymbol{X} = [\pm(T_0/T_1)^1 / \pm (T_0/T_1)^2 / \pm (T_0/T_1)^3 / \pm (T_0/T_1)^4]_S$$

where the superscript represents the ply of the laminate. A uniform average pressure is applied to all the panels. However, in the later cases, the linearly varying pressure is applied as shown in Fig. 8.

Case II: In this case, the top two layers of plies are optimized while the middle two ply layers are considered to be made of 90 deg.

$$\boldsymbol{X} = [\pm(T_0/T_1)^1 / \pm (T_0/T_1)^2 / (90/90)^3 / (90/90)^4]_S$$

Case III: In this case, the design variables are similar to the Case II. However, the actual variation of pressure distribution shown in Fig. 8 is used.

Case IV: The 15 panels of the skin is divided into three divisions in this case. The first divison corresponds to the five panels correspoinding to the skin panels near the D-spar. The second and third divsions corrspond to the next sets of panels. This case is used to study the optimal CVF corresponding to the varition of the pressure acting on the skin. Similar to Case II, the middle layers are fixed at 90 deg. The design variables of three sets of panels are given as

$$\boldsymbol{X_1} = [\pm(T_0/T_1)^1 / \pm (T_0/T_1)^2 / (90/90)^3 / (90/90)^4]_S$$
$$\boldsymbol{X_2} = [\pm(T_0/T_1)^1 / \pm (T_0/T_1)^2 / (90/90)^3 / (90/90)^4]_S$$
$$\boldsymbol{X_3} = [\pm(T_0/T_1)^1 / \pm (T_0/T_1)^2 / (90/90)^3 / (90/90)^4]_S$$

4.3 Optimal results:

A real coded genetic algorithm is used for the optimization[9]. The results for case I show T_0 and T_1 as 40 and 30 degs for the top layer which is less than 45 deg. However, the middle plies show the ply angles greater than 45 deg. The strain energy is significantly reduced and deflection is reduced to 30 %. This result shows that the plies which are away from the neutral axis tend to close to zero degrees so that the bending stiffness is increased or the maximum deflection is reduced.

Table 2. Optimal fibers of skin

Case	Optimal angles (degrees)	Percentage reduction (%)	
		J_1	J_2
I	X = [(40 /30) (60/ 60) (70/50) (70/50)]	7	30
II	X = [(40/40) (90/50)]	21	25
III	X = [(50/30)(50/80)]	19	20
IV	X_1 =[(30 /10) / (80/70)] X_2 =[(60 /30) / (50/70)] X_3 =[(60 /60) / (80/80)]	35	34

In case II, the optimal results show a reduction of 21% in the out-of-plane deflection whereas the strain energy shows a reduction of 25%. This shows that the plies closer to the neutral axis do not contribute significantly to minimizing the out-of-plane deflections. However, the plies near to the neutral axis of the laminate can significantly reduce the strain energy. The top plies show ply angles less than the 45 deg and the other plies are close to 90 deg. That is the top plies are used to minimize the deflection while the middle layers from the neutral axis are used to minimize the strain energy.

In cases III and IV, the pressure loading acting on the skin varies along the chord. The optimal ply angles for case III show optimal ply angles close to 50/30 deg for the top layer. Case IV shows a reduction of around 35% for strain energy and maximum deflection. This result shows that the optimal ply angles as [30/10] for the top plies close to the D-spar where the pressure is high compared to the panels near to the trailing edge. The optimal ply angles of panels near to the trailing edge are closer to 90 deg and hence this reduces the stiffness, and in turn the actuation energy required to deflect the skin to vary the camber.

5. CONCLUSION

In this study, a flexible skin for the variable camber rotor blade is studied with CVF composites. Initially, the skin of the morphing blade is modeled as plates supported between the D-spar and trailing edge of typical rotor blade dimensions. The CVF shows a 60 % increase in the in-plane to bending deformation ratio compared to the linear fibers. A variable camber internal structure structure is investigated for morphing rotor blade. The aerodynamic properties are calculated for the variable camber internal structure protype model developed. A fluid-structure interaction code is used to obtain the aerodynamic loads acting on the skin. The upper skin is then optimized to find the optimal curvilinear fiber paths. The ply angles between the stringers are optimized to minimize the strain energy required to deform the skin and minimize the maximum out-of-plane deflection. The optimal results show that the top plies play a significant role in minimizing the out-of-plane deflections. The plies near to the neutral axis of the laminate plays a considerable role in minimizing the strain energy. Further, the skin requires the stiff plies near the D-spar and flexible plies near the trailing edge as the pressure load decreases from the quarter chord to trailing edge portion of the airfoil. The numerical results show that the CVF composite skins can decouple and minimize the actuation energy requirements while simultaneously retaining the skin out-of-plane deformation requirements. Further requirements of the morphing skins such as the strain failure of fibers and the design of lower skins of the airfoil will be studied in the future.

ACKNOWLEDGEMENTS

This work is supported by the European Research Council through grant number 247045 entitled "Optimisation of Multi-scale Structures with Applications to Morphing Aircraft".

REFERENCES

[1] Reich, G.W., and Sanders, B. “Introduction to Morphing Aircraft Research,” Journal of Aircraft, 44(4), 2007.

[2] Barbarino, S., Bilgen, O., Ajaj, R. R., Friswell, M. I., Inman, D. J., “A Review of Morphing Aircraft”, Journal of Intelligent Material Systems and Structures, Vol. 22, (9). 2011.

[3] Gandhi, F., Frecker, M. and Nissly, A. “Design Optimization of a Controllable Camber Rotor Airfoil,” AIAA Journal, Vol. 46(1), 2008.

[4] Kerho, M. “Adaptive Airfoil Dynamic Stall Control,” Journal of Aircraft, Vol. 44(4), 2007.

[5] Thill, C., Etches, J., Bond, I., Potter, K. And Weaver, P. “Morphing Skins,” The Aeronautical Journal, 2008.

[6] Thuwis, G. A. A., Abdalla. M. M., and Gürdal, Z., “Optimization of a variable-stiffness skin for

morphing high-lift devices," Smart Materials and Structures, Vol 19 (12), 2010.

[7] Z. Gurdal, R. Olmedo, "In-plane response of laminates with spatially varying fbre orientations: variable stiffness concept," AIAA Journal, 31 (4) 1993.

[8] Woods, B.K.S., and Friswell, "Preliminary Investigation of a Fishbone Active Camber Concept," Proceedings of the ASME 2012 Conference on Smart Materials, Adaptive Structures and Intelligent Systems, September 19-21, 2012, Stone Mountain, GA.

[9] Murugan, MS and Suresh, S and Ganguli, R and Mani, V "Target vector optimization of composite box beam using real-coded genetic algorithm: a decomposition approach", Structural and Multidisciplinary Optimization, 33 (2). 2007.